Chemosphere 329 (2023) 138674

Contents lists available at ScienceDirect

Chemosphere

journal homepage: www.elsevier.com/locate/chemosphere

The ^{239}Pu nuclear fallout as recorded in an Antarctic ice core drilled at Dome C (East Antarctica)

Mirko Severi [a,b,*], Silvia Becagli [a,b], Laura Caiazzo [a,c], Raffaello Nardin [a,b], Alberto Toccafondi [d], Rita Traversi [a,b]

[a] Department of Chemistry "Ugo Schiff", University of Florence, Florence, Italy
[b] Institute of Polar Sciences, ISP-CNR, Venice-Mestre, Italy
[c] Ente per le Nuove Tecnologie, l'Energia e l'Ambiente, Rome, Italy
[d] Department of Information Engineering and Mathematics, University of Siena, Siena, Italy

HIGHLIGHTS

- Nuclear Weapons Tests were responsible of a global dispersion of radioactivity.
- Antarctic ice-cores preserve a detailed record of nuclear fallout.
- An ICP-MS method was successfully used to measure ^{239}Pu at fg g^{-1} level.
- The nuclear fallout can represent an useful tool for the dating of an ice-core.

GRAPHICAL ABSTRACT

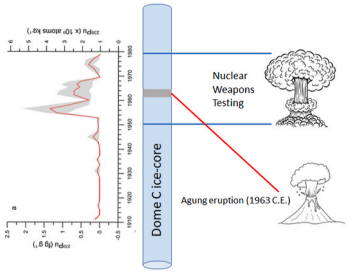

ARTICLE INFO

Handling Editor: Milena Horvat

Keywords:
Antarctica
Ice-cores
Nuclear fallout
Plutonium
ICP-MS

ABSTRACT

Starting from 1952 C.E. more than 540 atmospheric nuclear weapons tests (NWT) were conducted in different locations of the Earth. This lead to the injection of about 2.8 t of ^{239}Pu in the environment, roughly corresponding to a total ^{239}Pu radioactivity of 6.5 PBq. A semiquantitative ICP-MS method was used to measure this isotope in an ice core drilled in Dome C (East Antarctica). The age scale for the ice core studied in this work was built by searching for well-known volcanic signatures and synchronising these sulfate spikes with established ice core chronologies. The reconstructed plutonium deposition history was compared with previously published NWT records, pointing out an overall agreement. The geographical location of the tests was found to be an important parameter strongly affecting the concentration of ^{239}Pu on the Antarctic ice sheet. Despite the low yield of the tests conducted in the 1970s, we highlight their important role in the deposition of radioactivity in Antarctica due to the relative closeness of the testing sites.

1. Introduction

Since 20th century the global population and its capacity of changing nature have largely and rapidly increased. Deep changes in the Earth system arose from the higher use of resources and energy, from industrialization and from the global economic growth especially since the

* Corresponding author. Department of Chemistry "Ugo Schiff", University of Florence, Florence, Italy.
E-mail address: mirko.severi@unifi.it (M. Severi).

https://doi.org/10.1016/j.chemosphere.2023.138674
Received 23 January 2023; Received in revised form 4 April 2023; Accepted 10 April 2023
Available online 11 April 2023
0045-6535/© 2023 The Authors. Published by Elsevier Ltd. This is an open access article under the CC BY license (http://creativecommons.org/licenses/by/4.0/).

1950's, when the so-called Great Acceleration began (Steffen et al., 2007). Nowadays, the human species is known to be the major geomorphological force (Cooper et al., 2018) and its activities represent one of the strongest forcing factors directly affecting the on-going climatic change (IPCC, 2014). The discovery of nuclear fission in the late 1930s and its following development starting from Los Alamos in the 1940s, led to the beginning of the 'atomic age' with the release of radiogenic nuclides into the Earth's atmosphere and, hence, biosphere. This signature, recorded in several kind of climatic archives, has been proposed by many scientists as the event marking the onset of the "Anthropocene" (Sanchez-Cabeza et al., 2021). The radioactive chemical element plutonium (Pu) is present in the environment mainly as a consequence of the nuclear weapons testing (NWT) accomplished from 1945 to 1980 Common Era (C.E.) (UNSCEAR, 2000). Among the six isotopes of Pu (^{238}Pu, ^{239}Pu, ^{240}Pu, ^{241}Pu, ^{242}Pu and ^{244}Pu), ^{239}Pu is the most abundant in the environment with an half-life of 24,110 years. It is estimated that approximately 2.8 t of ^{239}Pu were globally deposited from the atmosphere as a result of more than 540 atmospheric weapons tests, corresponding to a total ^{239}Pu radioactivity of 6.5 PBq (UNSCEAR, 2000).

The radioactive fallout began in 1945 C.E (see Fig. 1). during World War II due to fission devices which were responsible of just local contamination. Thermonuclear weapon tests commenced in 1952 C.E. and were accomplished in three major phases. The first phase, from 1952 to 1958 C.E., was dominated by US testing at low latitude Pacific sites (Bikini, Eniwetok and Johnston Island). During this period, one of the largest tests, with a total yield of 15 Mt, was the Castle Bravo detonation at Bikini Atoll in 1954 C.E. This phase ended with the Partial Test Ban moratorium from November 1958–1961 C.E., a period characterized by a lull in nuclear weapon tests (NWT) except for three tests conducted by France. Phase two ranged between 1961 and 1963 C.E. and was dominated by the former Soviet Union (USSR) testing at Novaya Zemlya (Russian Arctic). At this site, the cumulated yield of the detonations conducted during phase two accounts for about 57% of all NWT carried out between 1945 and 1980 C.E. (UNSCEAR, 2000; Wendel et al., 2013; Arienzo et al., 2016). In 1963 C.E., the Limited Test Ban Treaty (LTBT) was signed by the U.S. and USSR. According to this agreement, NWT were banned in all global environments, except for the underground tests. Phase three of NWT lasted from 1963 to 1980 C.E. and was dominated by several above-ground test mainly conducted by France (Mururoa and Fangataufa Atolls – French Polynesia) and China (Lop Nor – western China).

The aerosols deriving from NWT can be dispersed on three different scales: local, regional (tropospheric) and global (stratospheric). Several factors can influence the partitioning of NWT aerosols (i.e. the yield and the height of the test, the test location and the local synoptic

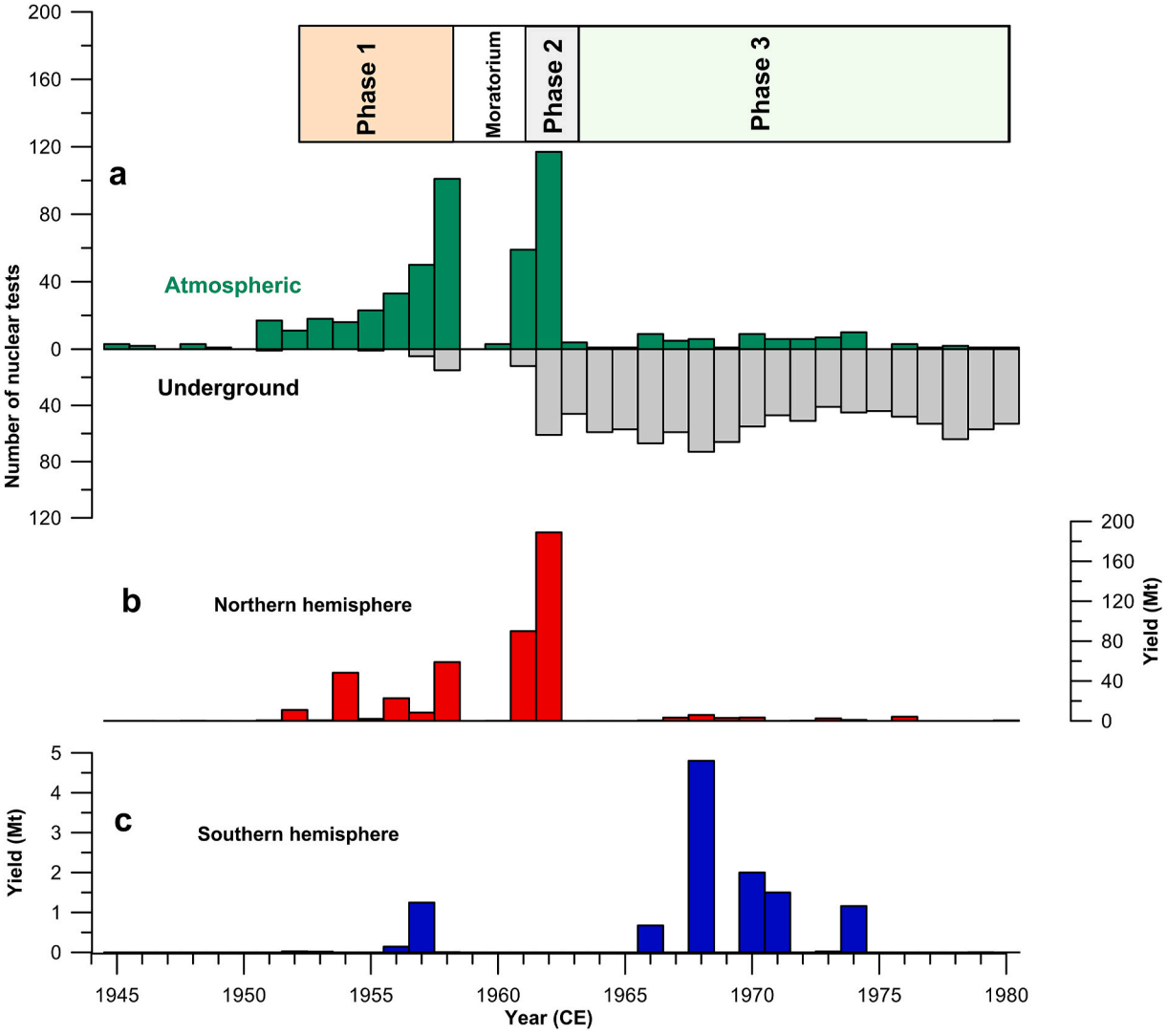

Fig. 1. (a) Number of atmospheric (green bars) and underground (grey bars) nuclear weapon tests run in each year during the studied period. (b–c) Northern and Southern Hemisphere atmospheric nuclear yields detonations in each year between 1945 and 1980 C.E.

meteorological conditions). These parameters can strongly influence the duration of the fallout, which can occur during periods ranging from minutes (on a local scale) to few years (for radionuclides reaching the stratosphere) (Alvarado et al., 2014). About 75–80% of global nuclear fallout occurred in the Northern Hemisphere (Livingston and Povinec, 2000), mostly in mid-latitudes (Waters et al., 2015) with minimum concentrations of radionuclides at the poles and in the equatorial region (Hardy et al., 1973).

In the last decades several tracers have been used to reconstruct the nuclear fallout coming from NWT (i.e. ^{3}H, ^{36}Cl, ^{90}Sr, ^{137}Cs, ^{210}Pb, ^{239}Pu, ^{240}Pu/^{239}Pu, beta-activity). Many kind of archives were analysed including vegetation (Warneke et al., 2002), dated corals (Benninger and Dodge, 1986; Lindahl et al., 2011; Sanchez-Cabeza et al., 2021), soil samples (Hardy et al., 1973; Roos et al., 1994), marine and lacustrine sediments (Krey et al., 1990; Roos et al., 1994), aerosol samples (Alvarado et al., 2014; Wendel et al., 2013), mid-latitude ice cores (Gabrieli et al., 2011; Olivier et al., 2004; Schwikowsky et al., 1999; Knusel et al., 2003; Wang et al., 2017) and polar ice cores (Arienzo et al., 2016; Hwang et al., 2019; Wendel et al., 2013; Koide et al., 1985; Winstrup et al., 2019). All these archives proved to be useful in reconstructing the history of nuclear fallout and, in particular, ice cores have been successfully used to achieve information on NWT aerosols deposition at high temporal resolution in the Arctic and in Antarctica (Fourre et al., 2006). Unlike beta-radiation-based methods, ^{239}Pu concentration in ice cores is stable through time, due to the long half-life (24.1 kyr) of this radionuclide. The main drawback in measuring this isotope is the low concentration (in the order of fg g^{-1}) usually found in ice cores which calls for sensitive instrumentation or large amount of samples. Typical methods for the analysis of Pu in ice cores are accelerator mass spectrometry (AMS) and inductively coupled plasma – sector field mass spectrometry (ICP-SFMS). AMS technique requires large amounts of snow or ice (2–3 kg per sample as reported by Olivier et al., 2004), whereas ICP-SFMS shows the great advantage of using just few mL of sample and does not require any sample pre-treatment (Arienzo et al., 2016; Gabrieli et al., 2011; Hwang et al., 2019). Besides being a proxy for the nuclear fallout reconstruction, ^{239}Pu could represent a key tool for dating purposes and to synchronize different ice-core records (Arienzo et al., 2016; Winstrup et al., 2019). In this study, we applied an ICP-SFMS method similar to those used by Gabrieli et al. (2011) and Hwang et al. (2019) on a shallow ice core drilled in Dome C (East Antarctica). ^{239}Pu concentration was successfully measured and compared with previous data achieved at several sites by ICP-SFMS or by radioactivity counting methods.

2. Materials and methods

2.1. Samples

During the 2018-19 Antarctic field campaign a 106 m long ice core (DC-3D) was drilled in Dome C (East Antarctica, 75°06′S; 123°21′E, 3233 m a.s.l) (Fig. 2) using an electromechanical drill in the framework of the MIUR-PNRA-3D project. The recent snow accumulation rate at Dome C ranged between 8.0 and 8.8 cm snow yr^{-1} in the period 1964–1992 CE (Traversi et al., 2009).

The ice core sections were logged and accurately weighted to evaluate the density of the snow. Afterwards, the ice core sections were cut in 10 cm sub-samples (roughly corresponding to a time resolution of 1–2 years in the analysed section) and each sub-sample was packed in a polyethylene bag, sealed and shipped to Italy at −20 °C.

The surface of the frozen samples was removed to clean the possible

Fig. 2. Ice cores or snow pits locations used for the study of the nuclear fallout in Antarctica. The red star shows the site in Dome C where the ice core of this study was drilled. Red circles show the six sites used by Arienzo et al. (2016) for the construction of a composite record: James Ross Island (JRI), B40, Aurora Basin North (ABN), Thwaites Glacier (THW), Pine Island Glacier (PIG) and the divide between Thwaites Glacier and Pine Island (DIV). Blue circles show other sites where the radioactive fallout was previously measured: Norwegian/U.S. traverse core site NUS_8_5, a site close to Dome C (Old Dome C), Dome Fuji, J-9 and Roosevelt Island Climate Evolution (RICE).

contamination inevitably arising from the drilling, cutting, packing and handling of the ice core. The decontamination technique used for the preparation of discrete samples was the manual removal of the outer layers using a ceramic knife under a laminar flow hood (Candelone et al., 1994). Decontaminated samples were than stored in pre-cleaned plastic containers and melted at room temperature in a class 10,000 laboratory just before the analysis.

2.2. Analytical methods

2.2.1. Electrical conductivity

A small amount (2 mL) of each sample was used for the measurement of the total conductivity; this parameter is often used as a marker, although not univocal, of acidic layers in ice cores due to the deposition of H_2SO_4 of volcanic origin. Due to the very low ionic strength of this kind of samples, this measurement is susceptible to atmospheric CO_2 absorption which, in turns, affects the measured total conductivity. For this reason, we used a Dionex CDM-3 conductivity flow cell with an active volume of 1.25 μL. Samples were pumped into the flow cell with a peristaltic pump (Minipulse 3, Gilson, Middleton, WI) at a flow rate of 0.5 mL min^{-1}, avoiding any contact with the laboratory atmosphere. Between 2.6 and 12.5 m depth, 95 samples covering the period from 1800 C.E. to 1980C.E. were analysed for the determination of their electrical conductivity and ionic composition.

2.2.2. Ion chromatography

Ion chromatographic analysis was performed on the ice core samples using a fully automated system described in details in Morganti et al. (2007). Briefly, two ion chromatographs (Thermo Dionex DX-500 and ICS-1000) were used for the determination of the anionic (Cl^-, NO_3^- and SO_4^{2-}) and cationic (Na^+, NH_4^+, K^+; Mg^{2+} and Ca^{2+}) species. Samples were injected into the ion chromatographic systems by using a 222 XL liquid handler automated sampler (Gilson, Middleton, WI, USA) able to pierce the sample vials with a stainless steel needle in order to minimise the sample handling and to avoid contact with the laboratory atmosphere. Standard solutions for calibrations were prepared daily by dilution of stock standard solutions (1000 mg L^{-1}) purchased from Merck (Darmstadt, Germany), with ultra-pure water (resistivity >18MΩ; Milli-Q IQ 7003, by Merck-Millipore). In this study, we focused on the use of non-sea-salt sulfate (nss-SO_4^{2-}) to detect historically known volcanic events with the purpose of building an age scale for the DC-3D ice core. Nss−SO_4^{2-} content was calculated by subtracting from total sulfate the contribution of primary sulfate (sea-salt sulfate) using ssNa^+ concentration as a univocal marker of the sea-spray source, as done by Severi et al. (2009).

2.2.3. ICP-SFMS

The determination of ^{239}Pu concentration was carried out using an ICP-SFMS (Element2, Thermo Scientific, Bremen, Germany) equipped with an high-efficiency sample introduction system (Apex HF, ESI, USA). Before the analysis all the samples were acidified at 1% (v/v) with ultra-pure HNO_3 obtained by a sub-boiling distillation system (Savillex DST-100, USA). Analyses were performed using a CETAC ASX-510 auto-sampler placed under a laminar flow hood Class 100 and a Teflon PFA self-aspirating microflow nebulizer (100 μL min^{-1}, Elemental Scientific, Omaha, NE, USA). The instrument was daily tuned in order to achieve the maximum sensitivity for the ^{115}In peak using a concentration of 100 pg mL^{-1}. ^{239}Pu concentration was measured in the low resolution (LR) mode with a mass resolution m/Δm ~ 300. Further details about optimised operational and instrumental parameters are summarised in Table 1 along with the main figures of merit of the method.

Since ^{239}Pu is a radioactive isotope, a standard reference material is not available; thus, an indirect calibration was performed using ^{238}U as an external standard (Gabrieli et al., 2011; Arienzo et al., 2016; Hwang et al., 2019). Considering that the sensitivity of heavy elements in ICP-SFMS is linked to their masses and that U and Pu have very similar first ionization energies, ^{238}U and ^{239}Pu are expected to show a similar behaviour in the plasma (Lariviere et al., 2006). In the last years, many studies have proved that this semi-quantitative approach for the determination of Pu is reliable and this method has been largely used in different matrices (Rondinella et al., 2000; Baglan et al., 2000; Arienzo et al., 2016; Winstrup et al., 2019). Standard solutions for U calibration were prepared by serial dilution of a 1000 μg mL^{-1} stock solution (Sigma Aldrich) in 1% (v/v) HNO_3 acidified ultrapure water. Five standard solutions ranging between 0.01 and 8.5 pg g^{-1} were daily prepared and measured at the beginning of every analysis session. In this working range, a linear calibration curve was obtained with R^2 always higher than 0.998.

Table 1
Set-up, main measurement parameters and figures of merit of our semi-quantitative ICP-SFMS for the determination of ^{239}Pu concentration.

Sampler/skimmer cones	Ni cones
Sample injector	Sapphire
Desolvation system	Apex-HF
Nebulizer	PFA microflow (100 μL min^{-1}) self-aspirating
Cool gas flow rate (L min^{-1})	16
Auxiliary gas flow rate (L min^{-1})	0.8 [a]
Sample gas flow rate (L min^{-1})	1.07 [a]
Rinse out time (min)	5
Sample take-up time (s)	90
RF power (W)	1268
Resolution	Low (m/Δm ~ 300)
Scan type	E-scan
Runs and passes	12 × 3
Sample per peak	100
Mass window (%)	20
Integration window (%)	20
Typical sensitivity	~0.8 × 10^6 cps for a 100 ng L^{-1} In solution
^{239}Pu LOD (fg g^{-1})	0.14
Background ^{239}Pu concentration (fg g^{-1})[b]	0.40

[a] These values were daily optimised during the instrument tuning.
[b] Average concentration between 1908 and 1942 C.E.

As reported in other studies (Gabrieli et al., 2011; Arienzo et al., 2016; Hwang et al., 2019), particular attention must be paid to the possible isobaric interference by $^{238}U^1H^+$. The separation between $^{238}U^1H^+$ and $^{239}Pu^+$ in a mass spectrometer would require a resolution better than 37,000 (Lariviere et al., 2006) and thus, using the low resolution mode (m/Δm ~ 300), we could just evaluate if the interference was negligible or not. By analysing different solutions of ^{238}U at concentrations ranging between 0.1 and 50 pg g^{-1}, we checked the hydride formation rate finding a mean $^{238}U^1H/^{238}U$ ratio of 8.1 × 10^{-5}. Since U concentrations were always lower than 1.0 pg g^{-1}, the contribution of $^{238}U^1H$ to the ^{239}Pu measurement was calculated to be always lower than 0.08 fg g^{-1}.

In order to rule out covariability between ^{238}U and ^{239}Pu, we evaluated their correlation in the period between 1945 and 1985 CE, finding a Pearson's r of 0.3064 (n = 24) which is statistically not significant. The method detection limit for ^{239}Pu, calculated as three times the standard deviation of ten measurement of the 1% (v/v) HNO_3, was 0.15 fg g^{-1}. A blank correction was applied to the full dataset by subtracting the average 1908–1942C.E. measured ^{239}Pu concentrations. The background concentration measured during this pre-atomic age in the DC-3D ice core was 0.40 fg g^{-1}. The precision of the method, expressed as RSD, ranged from 54 to 114% (mean 69%) for Pu concentrations higher than 0.5 fg g^{-1} while for concentrations lower than 0.5 fg g^{-1} precisions were from 17 to 173% (mean 90%). The uncertainty associated to each measurement was expressed as the relative standard deviation. A total of 41 samples between 2.6 and 6.9 m depth (covering the period between 1908 C.E. and 1980 C.E.) was analysed with this HR-ICP-MS semi-quantitative method.

2.3. Age-scale

A reliable age-scale represents a key tool for the correct interpretation of chemical profiles achieved from ice-cores. The full potential of climate archives can be exploited only when accurate dating models are available. A method often used for the construction of an age/depth model in ice archives is based on the counting of single annual layers deposited at the drilling site (Sigl et al., 2016; Nardin et al., 2021). This approach can be considered the best one for dating purposes but unfortunately it is applicable only to ice cores drilled at sites with a relatively high accumulation rate. When the identification of a seasonal pattern in the chemical or physical properties of ice is not possible, the use of ice flow models aided by the identification of temporal horizons (i.e. volcanic eruptions, magnetic anomalies or dust layers) represents the best dating strategy (Ruth et al., 2007). Due to the relatively low snow accumulation rate at Dome C and to the low sampling resolution used for the DC-3D core, the best approach to build an age scale for our record was a direct synchronisation with well dated ice cores. For this purpose, we used an ice core previously drilled in Dome C in the framework of the EPICA (European Project for Ice Coring in Antarctica) project in 1996/97 (hereafter EDC96). The uppermost section of this core was analysed in the field at high resolution by Fast Ion Chromatographic (FIC) methods (Severi et al., 2015; Traversi et al., 2002) and was already synchronised via volcanic stratigraphic links with several other records: EDML (Severi et al., 2007), Talos Dome (Severi et al., 2012), Vostok (Parrenin et al., 2012), Dome Fuji (Fujita et al., 2015) and WDC (Buizert et al., 2018). Since EDC96 core started from a depth of about 7 m (roughly corresponding to 1907C.E.), we used the more recent record by Gautier et al. (2016) to cover the more recent section. Fig. 3 shows the DC-3D, EDC96, Dome C and WDC sulfate profiles for the last two centuries after their synchronisation via the major historically known volcanic eruptions: Agung (1963 C.E.), Krakatoa (1884 C.E.), Cosiguina (1834 C.E.), Tambora (1815 C.E.) and an unknown volcano erupting in 1809 C.E. Despite the low resolution of the DC-3D ice core, these five volcanic horizons can be identified in the sulfate and conductivity profiles, allowing for an accurate chronology for our record. Since the time period on which we focused in this study is limited to the 1910–1980 C.E. interval, we can estimate a maximum uncertainty of 1–2 years for our chronology.

3. Results

Here we report the semiquantitative measurements of the ^{239}Pu concentration in the DC-3D ice core in the depth interval between 2.6 and 6.9 m, corresponding to a time period spanning from 1908 to 1980 C.E. The sample resolution used in the framework of the DC-3D project was 10 cm, we thus calculated an average time resolution of 1–2 years per sample. From the semiquantitative concentrations we calculated the ^{239}Pu results expressed in activity units as well, using the specific activity of 2.29 × 10^9 Bq g^{-1} for this isotope, as reported by Baglan et al.

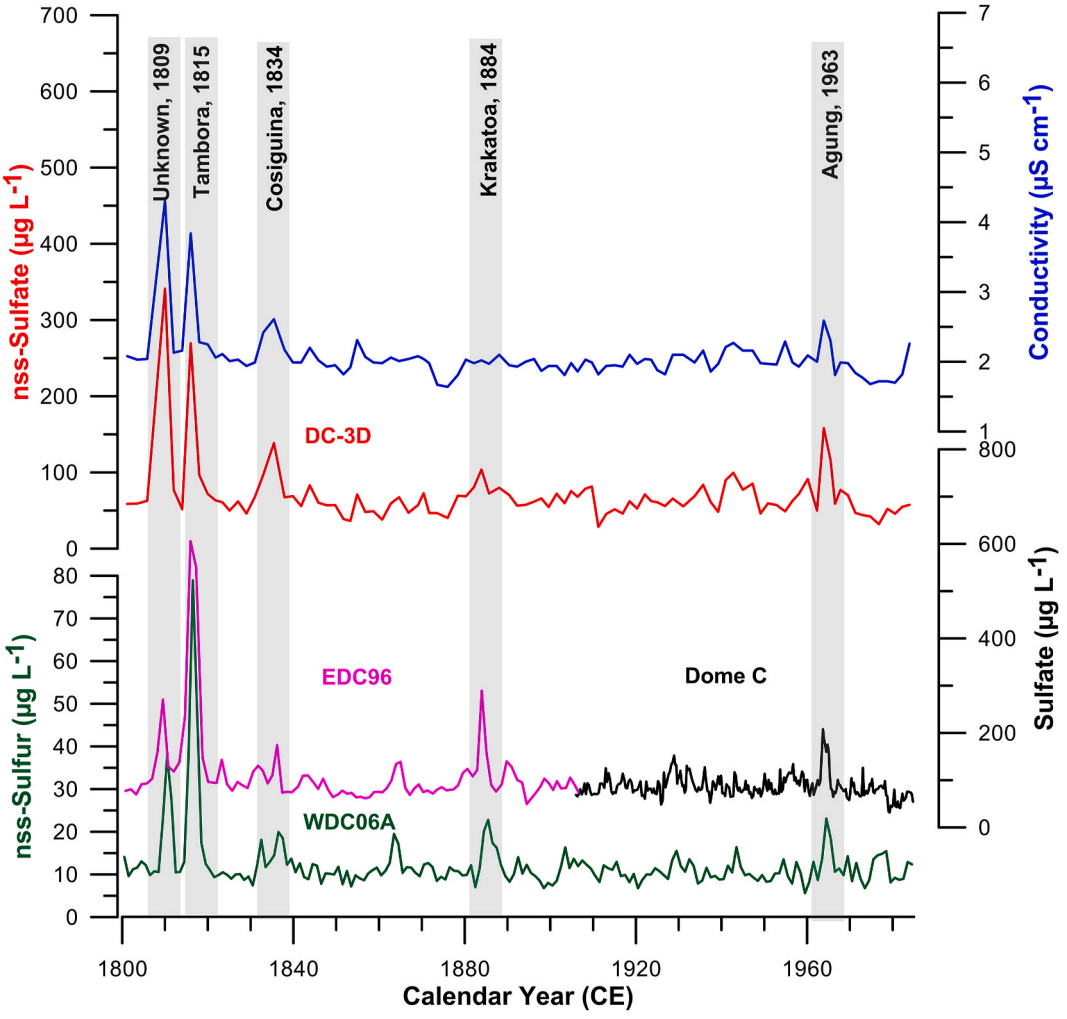

Fig. 3. Synchronisation of the DC-3D ice core with previous well-dated records using volcanic signatures during the last two centuries. The DC-3D liquid conductivity (blue line) and sulfate concentration (red line) have been plotted on the WDC age scale after their synchronisation with WDC sulfur concentration (green line – Sigl et al., 2015) and with EDC96 (purple) and EDC (Gautier et al., 2016) (black) sulfate profiles.

(2000). Fig. 4 shows the concentration profile of ^{239}Pu (panel a) and the activity profile (panel b) as recorded in the DC-3D ice core. From 1954 to 1957 C.E. a sharp increase in ^{239}Pu concentration and activity are observed. During this period the highest value of the whole dataset was recorded, with a maximum concentration of 1.35 fg g^{-1} in 1955–56 C.E. and an average concentration and activity of 1.12 fg g^{-1} and 2.56 mBq kg^{-1} respectively. After this ^{239}Pu peak, the concentration declined as a result of the Partial Test Ban moratorium (see Fig. 1); starting from 1961 C.E., a second concentration peak is clearly visible reaching its maximum between 1962 and 1968 C.E. After this peak, the ^{239}Pu concentration and activity returned close to background values during the 1970s as a consequence of the ban of atmospheric tests signed in 1963 C.E. by the U.S. and USSR.

4. Discussion

4.1. Comparison to atmospheric NWT history

In order to better understand the ^{239}Pu concentration profile obtained by using the semi-quantitative method, we compared our record to the total fission yield of NWT. The amount of Pu deposited on ice-sheets was mostly from atmospheric NWT, as underground NWT is expected to represent a negligible contribution to the total amount of ^{239}Pu deposited in polar areas. Atmospheric NWT eject debris into the stratosphere followed by wet or dry deposition within 1–2 years. For this reason, we calculated the cumulative yield for each year only taking into account the atmospheric tests and then we compared it with the ^{239}Pu concentration record according to our chronology, as shown in Fig. 5. Most of the NWT run in the Southern Hemisphere were carried out between 1966 and 1975 C.E. by France in the Southern Pacific Ocean (~21.8° S, ~139.0° W). The ^{239}Pu peak associated to this sequence of tests is clearly visible in the last part of our record between 1970 and 1977 C.E. The maximum concentration of ^{239}Pu is 0.31 fg g^{-1}; this value is much lower than the peaks recorded in 1962–63 C.E. (0.70 fg g^{-1}) and in 1954–55 C.E. (1.35 fg g^{-1}). The highest ^{239}Pu concentration (1954-55C.E.) can be explained as a consequence of the Mike and Bravo tests (UNSCEAR, 2000) run between 1952 and 1954 C.E. by the U.S. in a relatively close site in the South Pacific (~11°N). Despite a much lower nuclear yield (see Fig. 1), these NWT were responsible for a larger ^{239}Pu deposition with respect to the one due to the intensive testing in the Arctic (Novaya Zemlya, ~74°N) by the USSR in 1961–1962 C.E. Our results show that, as expected, the geographical location of the nuclear tests is not the only parameter affecting the amount of radionuclides deposited on the ice-sheets. In fact, the distance dependence of the

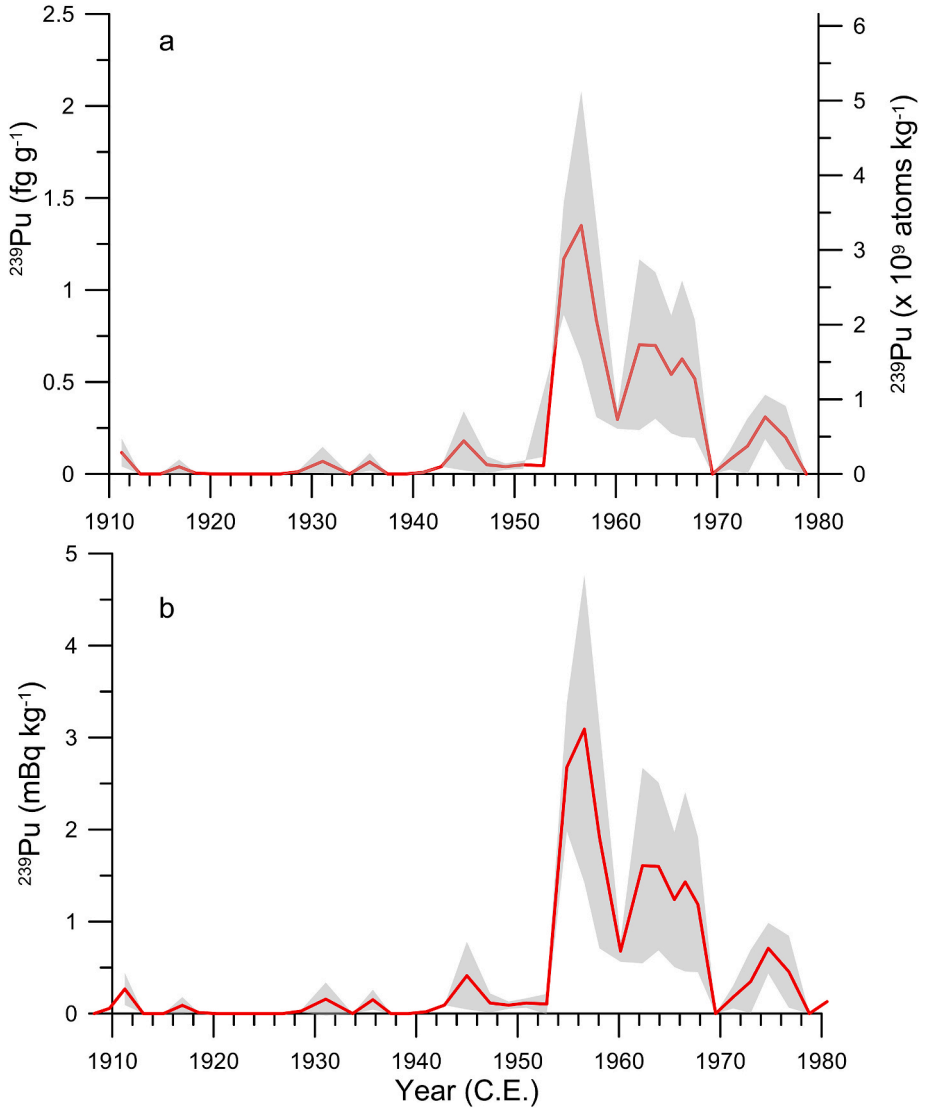

Fig. 4. Concentration profile of ^{239}Pu (panel a) and activity profile (panel b) as recorded in the DC-3D ice core. The shaded areas in both panels show the uncertainties arising from our semi-quantitative method.

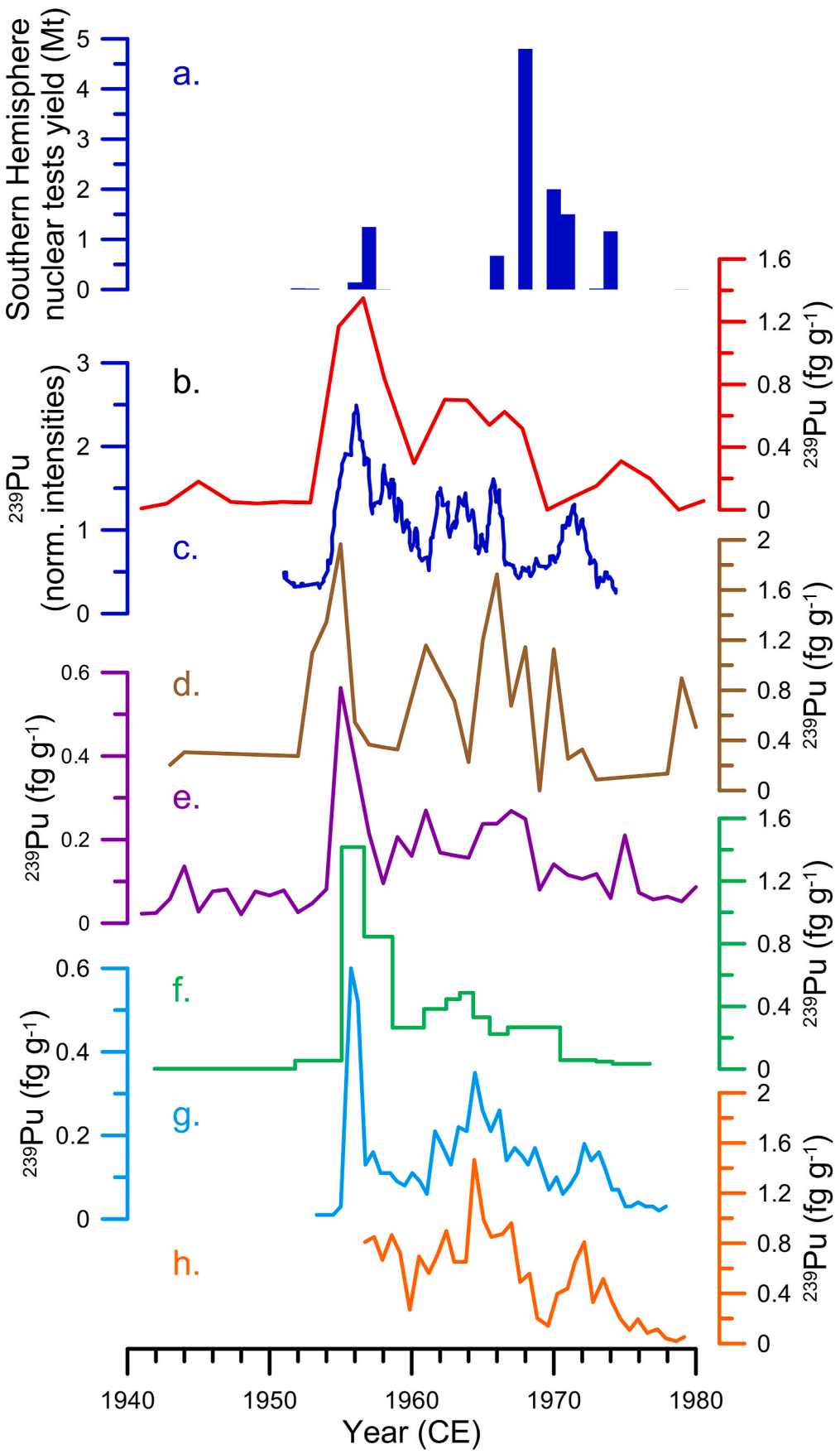

Fig. 5. Comparison between our ^{239}Pu concentration record and the other available records. (a) Yearly yield of southern hemisphere nuclear tests run between 1940 and 1980 C.E. (b) DC-3D semi-quantitative ^{239}Pu concentration (red), (c) RICE ^{239}Pu normalized intensities (blue – Winstrup et al., 2019), (d) NUS_8_5 ^{239}Pu concentration (brown- Arienzo et al., 2016)), (e) Antarctic composite record of ^{239}Pu concentration (purple- Arienzo et al., 2016)), (f) Old Dome C calculated ^{239}Pu concentration (green - Koide et al., 1979 and Koide et al., 1985), (g) J-9 calculated ^{239}Pu concentration plotted on the chronology proposed by Hwang et al. (2019) (light blue - Cutter et al., 1979 and Koide et al., 1985), (h) Dome Fuji snow-pit ^{239}Pu concentration (orange- Hwang et al., 2019).

transport of radionuclides holds true for the troposphere but it weakens for the stratospheric transport (Hwang et al., 2019), for which the residence time is expected to be 1.5 ± 0.5 years (Hirose and Povinec, 2015). In turn, the height reached by radioactive products after NWT depends on the yield of the nuclear test. It was observed that an explosion of tens to hundreds of kilotons produces a mushroom cloud that can reach an height close to the tropopause, while smaller tests can spread the radioactive products just in the troposphere (Hwang et al., 2019). It follows that the main factors affecting the deposition of Pu at a certain site are the geographical location of the NWT and its total yield, which can trigger a stratospheric distribution.

4.2. Comparison to other fallout records

A further evaluation of the dataset obtained using our method was carried out by a comparison with the available published records of nuclear fallout on the Antarctic ice sheet (see Fig. 2). Unfortunately, only few studies have been performed so far on Antarctic ice cores or snow-pits. In particular, we compared our record with:

1. A composite Antarctic record produced by Arienzo et al. (2016) obtained by calculating the geometric mean of six well dated ice-cores
2. An additional ice core analysed by Arienzo et al. (2016) at a site with an accumulation rate close to Dome C (NORUS_8_5, recent accumulation rate of 35 mm yr^{-1} water equivalent)
3. A 4 m snow pit dug close to Dome Fuji (Hwang et al., 2019)
4. An ice core drilled in Roosevelt Island in the framework of the RICE project (Winstrup et al., 2019)
5. A 6 m snow pit dug at J-9 in November 1976 (Cutter et al., 1979; Koide et al., 1985)
6. A 5 m snow pit dug at Old Dome C in January 1977 (Koide et al., 1979, 1985).

While in the first four records the history of NWT was reconstructed by measuring ^{239}Pu with an ICP-MS, the J-9 and Old Dome C snow pits studied in the 1970s were analysed by measuring the $^{239+240}$Pu activity on large samples by alpha spectrometry. In order to obtain the concentration of ^{239}Pu, we subtracted the contribution of ^{240}Pu from the total activity by using its specific activity (8.39×10^9 Bq g^{-1}; Baglan et al., 2000) and the different ^{240}Pu/^{239}Pu atomic ratios reported in Koide et al. (1985). Finally, we calculated the ^{239}Pu concentrations corresponding to the residual activity by using the ^{239}Pu specific activity of 2.29×10^9 Bq g^{-1} (Baglan et al., 2000). Fig. 5 shows the comparison of our new profile with the aforementioned records. All the records are plotted on their original age scale except for the J-9 snow pit, whose age scale was shifted by adding 2.1 years to the original chronology, as proposed by Hwang et al. (2019). We observe an overall agreement among the available ^{239}Pu concentration trends, with the highest values occurring between 1952 and 1956 C.E. After a low concentration period during the Moratorium, a second peak is visible between 1962 and 1968 C.E. This second peak reaches about half the concentration of the first one at each site. This concentration maximum is in turn followed by a third one showing slightly lower concentrations and starting in the early 1970s as a consequence of the French low-latitude nuclear weapons testing. Although this main pattern is common to all records, some differences appear when looking into details. Several issues affecting the plutonium records can preclude the possibility to link these differences to a spatiotemporal heterogeneity in the ^{239}Pu fallout. In fact, each record has an age uncertainty which could explain the lead or lag of the plutonium deposition with respect to other archives. Furthermore, the low accumulation rate at Dome C represents a drawback when studying archives at high resolution since the wind-driven reworking of snow can heavily disturb the stratigraphy of annual layers (Gautier et al., 2016). For these reasons it is not possible to discuss further about the spatiotemporal distribution of ^{239}Pu over Antarctica. In order to accomplish this task high resolution and accurately-dated records are mandatory. Finally, we evaluated the post-moratorium (1962–1965 C.E.) to pre-moratorium (1955–1959 C.E.) ratio for ^{239}Pu deposition by integrating the ^{239}Pu concentration during these two time intervals and calculating their ratio. On the basis of the total atmospheric NWT yields during these two periods, this ratio is about 70:30% (Koide et al., 1982). The ratio calculated in our DC-3D record is 37:63%, which is perfectly in agreement with the values of 36:64% and 38:62% found at Dome C (Koide et al., 1982) and in an Antarctic composite record (Arienzo et al., 2016) respectively. These ratios are rather offset from the expected post-moratorium to pre-moratorium ratio of 70:30%. This discrepancy can be explained considering that Pu is not a fission product and its production is strongly dependent on the type of weapon tested (Koide et al., 1982).

5. Conclusions

In this work we demonstrated the reliability of an ICP-SFMS method for the quantification of ^{239}Pu in an ice core drilled on the Antarctic Plateau. The only isobaric interference ($^{238}UH^+$) was found to be negligible at this site, but caution must be used at sites with high dust content since high U concentrations are to be expected. Our semi-quantitative method allowed us to reconstruct the nuclear fallout deposition between 1940 and 1980 C.E., representing a useful tool for building chronologies for ice cores difficult to date. The obtained results were compared with existing ^{239}Pu records pointing out a good overall agreement among ice cores drilled at different sites across the Antarctic continent. The new ^{239}Pu deposition data at Dome C represent a valuable information to better understand the mechanisms involved in the transport processes of aerosol towards high latitudes. For instance, assuming a similar behaviour between volcanic sulfate injected into the stratosphere and the radioactivity coming from bomb tests, this Pu concentration profile could be used to better model the forcing exerted by volcanic aerosol on a global scale (Sigl et al., 2022).

Author statement

Mirko Severi: Conceptualization, Formal analysis, Writing – original draft, Writing – review & editing, Project administration, Funding acquisition. **Silvia Becagli**: Formal analysis, Methodology, Writing – review & editing. **Laura Caiazzo**: Formal analysis, Methodology, Writing – review & editing. **Raffaello Nardin**: Formal analysis, Methodology, Writing – review & editing. **Alberto Toccafondi**: Project administration, Funding acquisition, Writing – review & editing. **Rita Traversi**: Formal analysis, Methodology, Writing – review & editing.

Declaration of competing interest

The authors declare that they have no known competing financial interests or personal relationships that could have appeared to influence the work reported in this paper

Data availability

The data is available as supplementary table.

Acknowledgments

This research was financially supported by the 2016 Italian National Antarctic Program (MIUR- PNRA) in the framework of the PNRA 2016/AC3.05 project. This research was also funded by the Italian Ministry of University and Research (MIUR) within the framework of the project "Innovative Analytical Methods to study biogenic and anthropogenic proxies in Ice Cores" AMICO (MIUR-PRIN 2017). The field operations benefited from the support of the French-Italian Concordia Station. This work was also partially supported by Ente Cassa di Risparmio di Firenze

(ECRF). M.S., R.T. and S. B. thank MIUR-Italy ("Progetto Dipartimenti di Eccellenza 2018–2022" allocated to Department of Chemistry "Ugo Schiff"). We thank M. Pasquale and A. Verrocchi for their help in the cold room operations and in the IC analysis. We would also like to acknowledge the Norwegian Polar Institute for the use of the Qantarctica package, used to draw the map in Fig. 2.

Appendix A. Supplementary data

Supplementary data to this article can be found online at https://doi.org/10.1016/j.chemosphere.2023.138674.

References

Alvarado, J., Steinmann, P., Estier, S., Bochud, F., Haldimann, M., Froidevaux, P., 2014. Anthropogenic radionuclides in atmospheric air over Switzerland during the last few decades. Nat. Commun. 5 (3030), 1–6.

Arienzo, M.M., McConnell, J.R., Chellman, N., Criscitiello, A.S., Curran, M., Fritzsche, D., Kipfstuhl, S., Mulvaney, R., Nolan, M., Opel, T., Sigl, M., Steffensen, J.P., 2016. A method for continuous ^{239}Pu determinations in Arctic and Antarctic ice cores. Environ. Sci. Technol. 50, 7066–7073.

Baglan, N., Cossonnet, C., Pitet, P., Cavadore, D., Exmelin, L., Berard, P., 2000. On the use of ICP-MS for measuring plutonium in urine. J. Radioanal. Nucl. Chem. 243, 397–401.

Benninger, L., Dodge, R., 1986. Fallout plutonium and natural radionuclides in annual bands of the coral Montastrea annularis, St. Croix, U.S. Virgin Islands. Geochem. Cosmochim. Acta 50 (12), 2785–2797.

Buizert, C., Sigl, M., Severi, M., Markle, B.R., Wettstein, J.J., McConnell, J.R., Pedro, J.B., Sodemann, H., Goto-Azuma, K., Kawamura, K., Fujita, S., Motoyama, H., Hirabayashi, M., Uemura, R., Stenni, B., Parrenin, F., He, F., Fudge, T.J., Steig, E.J., 2018. Abrupt ice-age shifts in southern westerly winds and Antarctic climate forced from the north. Nature 563, 681–685.

Candelone, J.-P., Hong, S., Boutron, C.F., 1994. Anal. Chim. Acta 299 (1), 9–16.

Cooper, A.H., Brown, T.J., Price, S.J., Ford, J.R., Waters, C.N., 2018. Humans are the most significant global geomorphological driving force of the 21st century. Anthropocene Rev. 5 (3), 222–229.

Cutter, G.A., Bruland, K.W., Risebrough, R.W., 1979. Deposition and accumulation of plutonium isotopes in Antarctica. Nature 279, 628–629.

Fourre, E., Jean-Baptiste, P., Dapoigny, A., Baumier, D., Petit, J., Jouzel, J., 2006. Past and recent tritium levels in Arctic and Antarctic polar caps. Earth Planet Sci. Lett. 245 (1−2), 56–64.

Fujita, S., Parrenin, F., Severi, M., Motoyama, H., Wolff, E.W., 2015. Volcanic synchronization of Dome Fuji and Dome C Antarctic deep ice cores over the past 216 kyr. Clim. Past 11, 1395–1416. https://doi.org/10.5194/cp-11-1395-2015.

Gabrieli, J., Cozzi, G., Vallelonga, P., Schwikowski, M., Sigl, M., Eickenberg, J., Wacker, L., Boutron, C., Gaggeler, H., Cescon, P., Barbante, C., 2011. Contamination of Alpine snow and ice at Colle Gnifetti, Swiss/Italian Alps, from nuclear weapons tests. Atmos. Environ. 45 (3), 587–593.

Gautier, E., Savarino, J., Erbland, J., Lanciki, A., Possenti, P., 2016. Variability of sulfate signal in ice core records based on five replicate cores. Clim. Past 12, 103–113. https://doi.org/10.5194/cp-12-103-2016.

Hardy, E., Krey, P., Volchok, H., 1973. Global inventory and distribution of fallout plutonium. Nature 241 (5390), 444–445.

Hirose, K., Povinec, P.P., 2015. Source of plutonium in the atmosphere and stratosphere troposphere mixing. Sci. Rep. 5, 15707.

Hwang, H., Hur, S.D., Lee, J., Han, Y., Hong, S., Motoyama, H., 2019. Plutonium fallout reconstructed from an Antarctic Plateau snowpack using inductively coupled plasma sector field mass spectrometry. Sci. Total Environ. 669, 505–511. https://doi.org/10.1016/j.scitotenv.2019.03.105.

Intergovernmental Panel on Climate Change, 2014. Climate Change 2013 – the Physical Science Basis: Working Group I Contribution to the Fifth Assessment Report of the Intergovernmental Panel on Climate Change. Cambridge University Press, Cambridge. https://doi.org/10.1017/CBO9781107415324.

Knusel, S., Ginot, P., Schotterer, U., Schwikowski, M., Gaggeler, H., Francou, B., Petit, J., Simoes, J., Taupin, J., 2003. Dating of two nearby ice cores from the Illimani, Bolivia. J. Geophys. Res. 108 (D6), 1–11.

Koide, M., Michel, R., Goldberg, E.D., 1979. Depositional history of artificial radionuclides in the Ross ice shelf. Antarctica. Earth Planet Sci. Lett. 44, 204–223.

Koide, M., Michel, R., Goldberg, E.D., Herron, M.M., Langway, C.C., 1982. Characterization of radioactive fallout from pre- and post-moratorium tests to polar ice caps. Nature 296, 544–547.

Koide, M., Bertine, K., Chow, T., 1985. Goldberg, E. The ^{240}Pu/^{239}Pu ratio, a potential geochronometer. Earth Planet Sci. Lett. 72 (1), 1–8.

Krey, P.W., Heit, M., Livingston, H.D., Miller, K.M.J., 1990. Radioanal. Nucl. Chem. 138, 385–406.

Lariviere, D., Taylor, V.F., Evans, R.D., Cornett, R.J., 2006. Radionuclide determination in environmental samples by inductively coupled plasma mass spectrometry. Spectrochim. Acta Part B At. Spectrosc. 61, 877–904.

Lindahl, P., Asami, R., Iryu, Y., Worsfold, P., Keith-Roach, M., Choi, M., 2011. Sources of plutonium to the tropical Northwest Pacific Ocean (1943−1999) identified using a natural coral archive. Geochem. Cosmochim. Acta 75 (5), 1346–1356.

Livingston, H.D., Povinec, P.P., 2000. Anthropogenic marine radioactivity. Ocean Coast Manag. 43 (8–9), 689–712. https://doi.org/10.1016/S0964-5691(00)00054-5.

Morganti, A., Becagli, S., Castellano, E., Severi, M., Traversi, R., Udisti, R., 2007. An improved flow analysis-ion chromatography method for determination of cationic and anionic species at trace levels in Antarctic ice cores. Anal. Chim. Acta 603, 190–198. https://doi.org/10.1016/j.aca.2007.09.050.

Nardin, R., Severi, M., Amore, A., Becagli, S., Burgay, F., Caiazzo, L., Ciardini, V., Dreossi, G., Frezzotti, M., Hong, S.-B., Khan, I., Narcisi, B.M., Proposito, M., Scarchilli, C., Selmo, E., Spolaor, A., Stenni, B., Traversi, R., 2021. Dating of the GV7 East Antarctic ice core by high-resolution chemical records and focus on the accumulation rate variability in the last millennium. Clim. Past 17, 2073–2089. https://doi.org/10.5194/cp-17-2073-2021.

Olivier, S., Bajo, S., Fifield, L., Gaggeler, H., Papina, T., Santschi, P., Schotterer, U., Schwikowski, M., Wacker, L., 2004. Plutonium from global fallout recorded in an ice core from the Belukha glacier, Siberian Altai. Environ. Sci. Technol. 38 (24), 6507–6512.

Parrenin, F., Petit, J.-R., Masson-Delmotte, V., Wolff, E., Basile-Doelsch, I., Jouzel, J., Lipenkov, V., Rasmussen, S.O., Schwander, J., Severi, M., Udisti, R., Veres, D., Vinther, B.M., 2012. Volcanic synchronisation between the EPICA Dome C and Vostok ice cores (Antarctica) 0–145 kyr BP. Clim. Past 8, 1031–1045. https://doi.org/10.5194/cp-8-1031-2012.

Rondinella, V.V., Betti, M., Bocci, F., Hiernaut, T., Cobos, J., 2000. IC-ICP-MS applied to the separation and determination of traces of plutonium and uranium in aqueous leachates and acid rinse solutions of UO_2 doped with ^{238}Pu. Microchem. J. 67, 310–324.

Roos, P., Holm, E., Persson, R., Aarkrog, A., Nielsen, S., 1994. Deposition of ^{210}Pb, ^{137}Cs, $^{239+240}$Pu, ^{238}Pu, and ^{241}Am in the Antarctic Peninsula area. J. Environ. Radioact. 24, 235–251.

Ruth, U., Barnola, J.-M., Beer, J., Bigler, M., Blunier, T., Castellano, E., Fischer, H., Fundel, F., Huybrechts, P., Kaufmann, P., Kipfstuhl, S., Lambrecht, A., Morganti, A., Oerter, H., Parrenin, F., Rybak, O., Severi, M., Udisti, R., Wilhelms, F., Wolff, E., 2007. EDML1": a chronology for the EPICA deep ice core from Dronning Maud Land, Antarctica, over the last 150 000 years. Clim. Past 3, 475–484. https://doi.org/10.5194/cp-3-475-2007.

Sanchez-Cabeza, J.-A., Rico-Esenaro, S., Corcho-Alvarado, J., Röllin, S., Carricart-Ganivet, J., Montagna, P., Ruiz-Fernández, A., Cearreta, A., 2021. Plutonium in coral archives: a good primary marker for an Anthropocene type section. Sci. Total Environ. 771, 145077.

Schwikowski, M., Brutsch, S., Gaggeler, H., Schotterer, U., 1999. A high-resolution air chemistry record from an Alpine ice core: Fiescherhorn glacier, Swiss Alps. J. Geophys. Res. Atmos. 104 (D11), 13709–13719.

Severi, M., Becagli, S., Castellano, E., Morganti, A., Traversi, R., Udisti, R., Ruth, U., Fischer, H., Huybrechts, P., Wolff, E., Parrenin, F., Kaufmann, P., Lambert, F., Steffensen, J.P., 2007. Synchronisation of the EDML and EDC ice cores for the last 52 kyr by volcanic signature matching, Clim. Past 3, 367–374. https://doi.org/10.5194/cp-3-367-2007.

Severi, M., Becagli, S., Castellano, E., Morganti, A., Traversi, R., Udisti, R., 2009. Thirty years of snow deposition at Talos Dome (Northern Victoria Land, East Antarctica): chemical profiles and climatic implications. Microchem. J. 92, 15–20.

Severi, M., Udisti, R., Becagli, S., Stenni, B., Traversi, R., 2012. Volcanic synchronisation of the EPICA-DC and TALDICE ice cores for the last 42 kyr BP. Clim. Past 8, 509–517. https://doi.org/10.5194/cp-8-509-2012.

Severi, M., Becagli, S., Traversi, R., Udisti, R., 2015. Recovering paleo-records from Antarctic ice-cores by coupling a continuous melting device and fast ion chromatography. Anal. Chem. 87, 11441–11447.

Sigl, M., Winstrup, M., McConnell, J.R., Welten, K.C., Plunkett, G., Ludlow, F., Büntgen, U., Caffee, M., Chellman, N., Dahl-Jensen, D., Fischer, H., Kipfstuhl, S., Kostick, C., Maselli, O.J., Mekhaldi, F., Mulvaney, R., Muscheler, R., Pasteris, D.R., Pilcher, J.R., Salzer, M., Schüpbach, S., Steffensen, J.P., Vinther, B.M., Woodruff, T. E., 2015. Timing and climate forcing of volcanic eruptions for the past 2,500 years. Nature 523, 543–549.

Sigl, M., Fudge, T.J., Winstrup, M., Cole-Dai, J., Ferris, D., McConnell, J.R., Taylor, K.C., Welten, K.C., Woodruff, T.E., Adolphi, F., Bisiaux, M., Brook, E.J., Buizert, C., Caffee, M.W., Dunbar, N.W., Edwards, R., Geng, L., Iverson, N., Koffman, B., Layman, L., Maselli, O.J., McGwire, K., Muscheler, R., Nishiizumi, K., Pasteris, D.R., Rhodes, R.H., Sowers, T.A., 2016. The WAIS Divide deep ice core WD2014 chronology – Part 2: annual-layer counting (0–31 ka BP). Clim. Past 12, 769–786. https://doi.org/10.5194/cp-12-769-2016.

Sigl, M., Toohey, M., McConnell, J.R., Cole-Dai, J., Severi, M., 2022. Volcanic stratospheric sulfur injections and aerosol optical depth during the Holocene (past 11 500 years) from a bipolar ice-core array. Earth Syst. Sci. Data 14, 3167–3196. https://doi.org/10.5194/essd-14-3167-2022.

Steffen, W., Crutzen, P.J., McNeill, J.R., 2007. The Anthropocene: are humans now overwhelming the great forces of nature. AMBIO A J. Hum. Environ. 36 (8), 614–621. https://doi.org/10.1579/0044-7447(2007)36[614. TAAHNO]2.0.CO;2.

Traversi, R., Becagli, S., Castellano, E., Migliori, A., Severi, M., Udisti, R., 2002. High resolution Fast Ion Chromatography (FIC) measurements of chloride, nitrate and sulfate along the EPICA Dome C ice core. Ann. Glaciol. 35, 291–298.

Traversi, R., Becagli, S., Castellano, E., Cerri, O., Morganti, A., Severi, M., Udisti, R., 2009. Study of Dome C site (East Antartica) variability by comparing chemical stratigraphies. Microchem. J. 92, 7–14.

UNSCEAR, 2000. Annex C: exposures to the public from man-made sources of radiation. In: Sources and Effects of Ionizing Radiation (Vienna).

Wang, C., Hou, S., Pang, H., Liu, Y., Gäggeler, H.W., Christl, M., Synal, H.-A., 2017. ^{239,240}Pu and ^{236}U records of an ice core from the eastern Tien Shan (Central Asia). J. Glaciol. 63 (241), 929–935.

Warneke, T., Croudace, I., Warwick, P., Taylor, R., 2002. A new ground-level fallout record of uranium and plutonium isotopes for northern temperate latitudes. Earth Planet Sci. Lett. 203 (3–4), 1047–1057.

Waters, C.N., Syvitski, J.P., Gałuszka, A., Hancock, G.J., Zalasiewicz, J., Cearreta, A., Grinevald, J., Catherine, J., McNeill, J.R., Summerhayes, C., Barnosky, A., 2015. Can nuclear weapons fallout mark the beginning of the Anthropocene Epoch? Bull. At. Sci. 71 (3), 46–57. https://doi.org/10.1177/0096340215581357.

Wendel, C.C., Oughton, D.H., Lind, O.C., Skipperud, L., Fifield, L.K., Isaksson, E., Tims, S. G., Salbu, B., 2013. Chronology of Pu isotopes and 236U in an Arctic ice core. Sci. Total Environ. 461–462, 734–741.

Winstrup, M., Vallelonga, P., Kjær, H.A., Fudge, T.J., Lee, J.E., Riis, M.H., Edwards, R., Bertler, N.A.N., Blunier, T., Brook, E.J., Buizert, C., Ciobanu, G., Conway, H., Dahl-Jensen, D., Ellis, A., Emanuelsson, B.D., Hindmarsh, R.C.A., Keller, E.D., Kurbatov, A.V., Mayewski, P.A., Neff, P.D., Pyne, R.L., Simonsen, M.F., Svensson, A., Tuohy, A., Waddington, E.D., Wheatley, S., 2019. A 2700-year annual timescale and accumulation history for an ice core from Roosevelt Island, West Antarctica, Clim. Past 15, 751–779. https://doi.org/10.5194/cp-15-751-2019.